Supporting Information

The Role of Connectivity on Electronic Properties of Lead Iodide Perovskite-Derived Compounds

Machteld E. Kamminga,[†] *Gilles A. de Wijs,*[‡] *Remco W. A. Havenith,* [†,§,⊥] *Graeme R. Blake,* [†] *Thomas T.M. Palstra**,[†]

[†]Zernike Institute for Advanced Materials and [§]Stratingh Institute for Chemistry, University of Groningen, Nijenborgh 4, 9747 AG Groningen, The Netherlands

[‡]Radboud University, Institute for Molecules and Materials, Heyendaalseweg 135, 6525 AJ Nijmegen, The Netherlands

[⊥]Ghent Quantum Chemistry Group, Department of Inorganic and Physical Chemistry, Ghent University, Krijgslaan 281 (S33), B-9000 Gent, Belgium

* E-mail: t.t.m.palstra@rug.nl, present address: University of Twente, The Netherlands

Figure S1. Photograph of the three types of crystals obtained: *bright orange* platelets ((C$_6$H$_5$CH$_2$NH$_3$)$_2$PbI$_4$), *colorless* needles (an unidentified phase), and *nearly transparent, light yellow* bar-shaped crystals ((C$_6$H$_5$CH$_2$NH$_3$)$_4$Pb$_5$I$_{14}$·2H$_2$O).
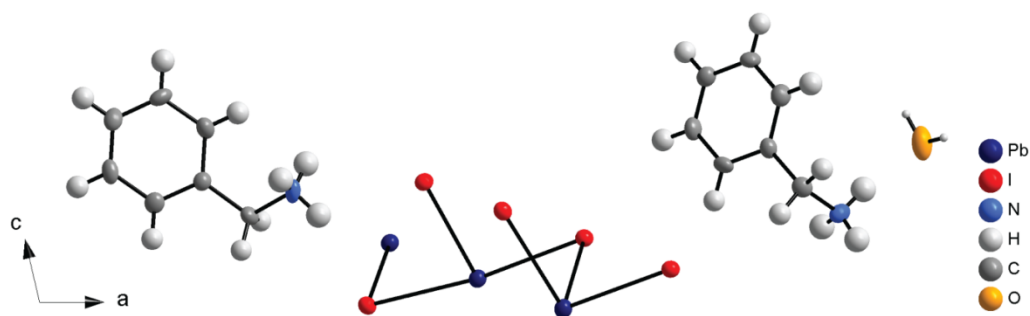
Figure S2. Asymmetric unit of (C$_6$H$_5$CH$_2$NH$_3$)$_4$Pb$_5$I$_{14}$·2H$_2$O at 100 K, showing thermal ellipsoids at 50% probability. The H$_2$O molecules are rotationally disordered and the orientation drawn should be considered illustrative only.
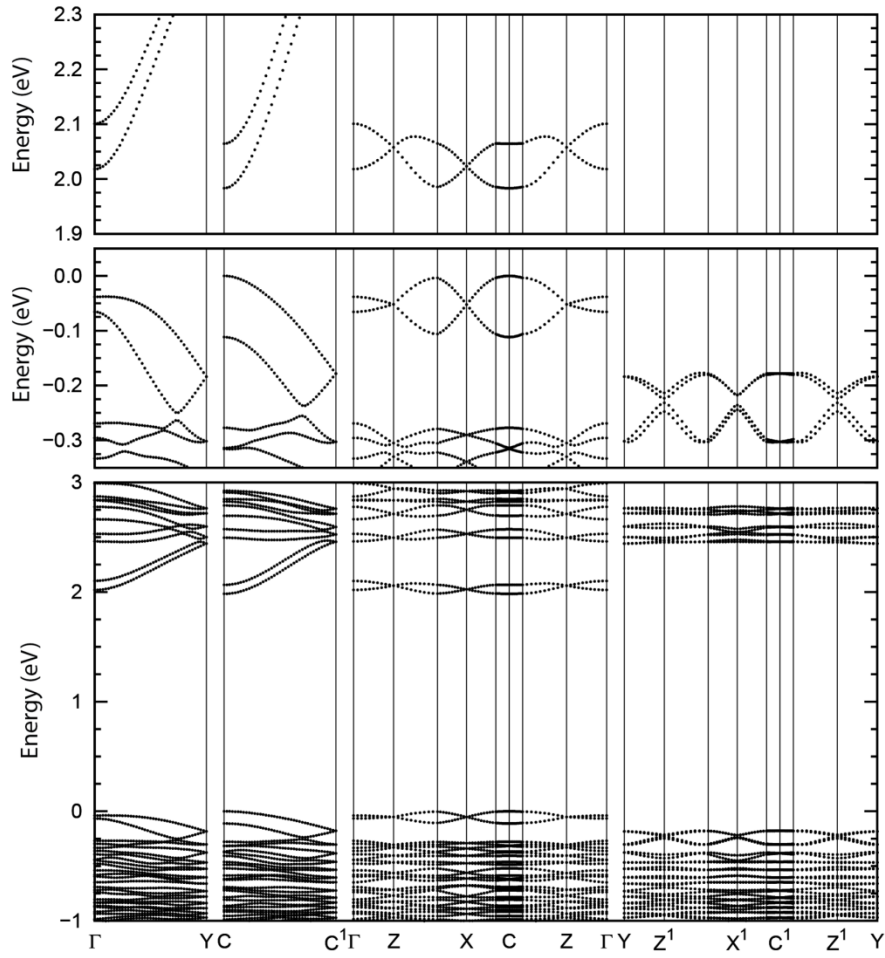
Figure S3. Extended version of the band structure of $(C_6H_5CH_2NH_3)_4Pb_5I_{14}$ within PBE-DFT+SOC, with $\Gamma = (0, 0, 0)$, $X = (0.5, 0, 0)$, $Y = (0, 0.5, 0)$, $Z = (0, 0, 0.5)$ and $C = (0.5, 0, 0.5)$ or equivalent $(0.5, 0, -0.5)$. The superscript "1" denotes addition of $(0, 0.5, 0)$. The coordinates denote multiples of the reciprocal lattice basis vectors $a*$, $b*$ and $c*$, respectively.
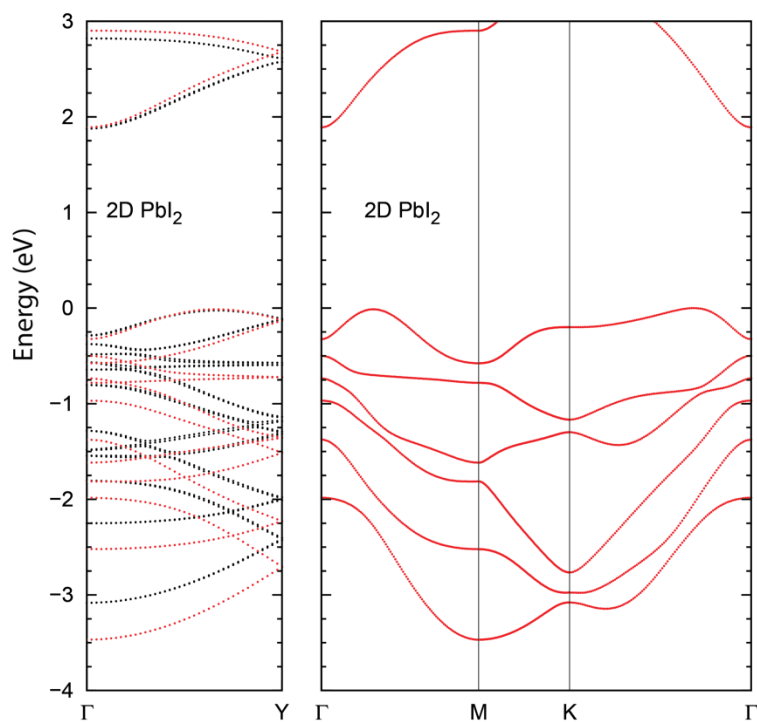
Figure S4. Band structure of a 2D PbI$_2$ sheet within PBE-DFT+SOC. The left panel reproduced Figure 4 (c), showing band structures of a 2D PbI$_2$ sheet built from the experimental atomic positions (black) and of an idealized edge-sharing slab with fixed Pb-I distances of 3.15 Å (red). The right panel shows a more elaborate band structure of the idealized edge-sharing slab, as calculated for a hexagonal unit cell, over the hexagonal Brillouin zone path.

Exploring the effect that edge-sharing of PbI$_6$ octahedra has on the dispersion using a tight-binding (TB) approximation.

It is important to mention that there are two different structural motifs that can be built from edge-sharing octahedra, as shown in Figure S5. One possibility has hexagonal symmetry, in which each Pb ion has six nearest neighbors, linked by 90° Pb-I-Pb angles only. This is the type of edge-sharing we encounter in $(C_6H_5CH_2NH_3)_4Pb_5I_{14} \cdot 2H_2O$ and is therefore discussed here. The other possibility has tetragonal symmetry, in which each Pb ion is linked to four nearest neighbors by 90° Pb-I-Pb angles via shared edges and to four next-nearest neighbors by 180° Pb-I-Pb angles via shared corners.
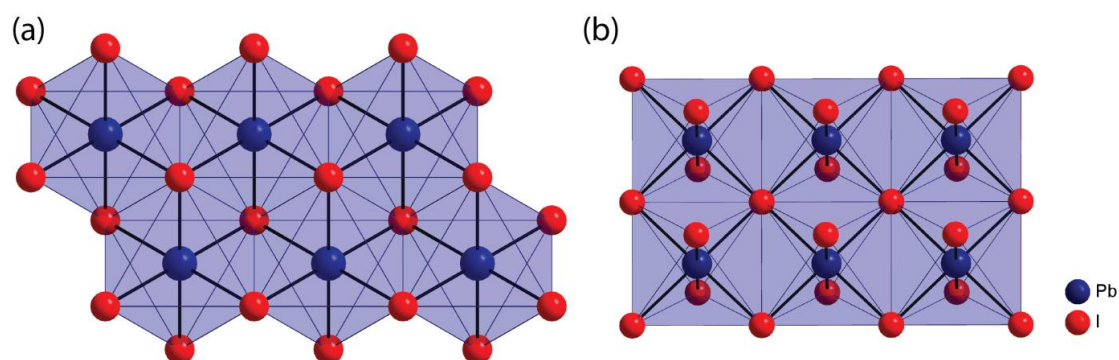
Figure S5. Comparison of two types of edge-sharing. (a) Hexagonal, with all Pb-I-Pb angles 90°. (b) Tetragonal, with Pb-I-Pb angles of 90° for edge-shared octahedra and 180° for corner-sharing octahedra.

Thus, the hexagonal model is the only case in which solely edge-sharing occurs and is therefore the model we use to compare edge-sharing with corner-sharing. Consequently, we studied the band structure of two theoretical model structures: a 3D structure solely consisting of corner-sharing PbI$_6$-octahedra and the 2D edge-sharing structure of which the band structure is given in Figure S4. These are simplified structural models, in which all the Pb-I distances are fixed to 3.15 Å, and octahedral tilting is absent. Figure S6 shows the band structures of both structure models, as well as a tight-binding (TB) fit to the calculations.
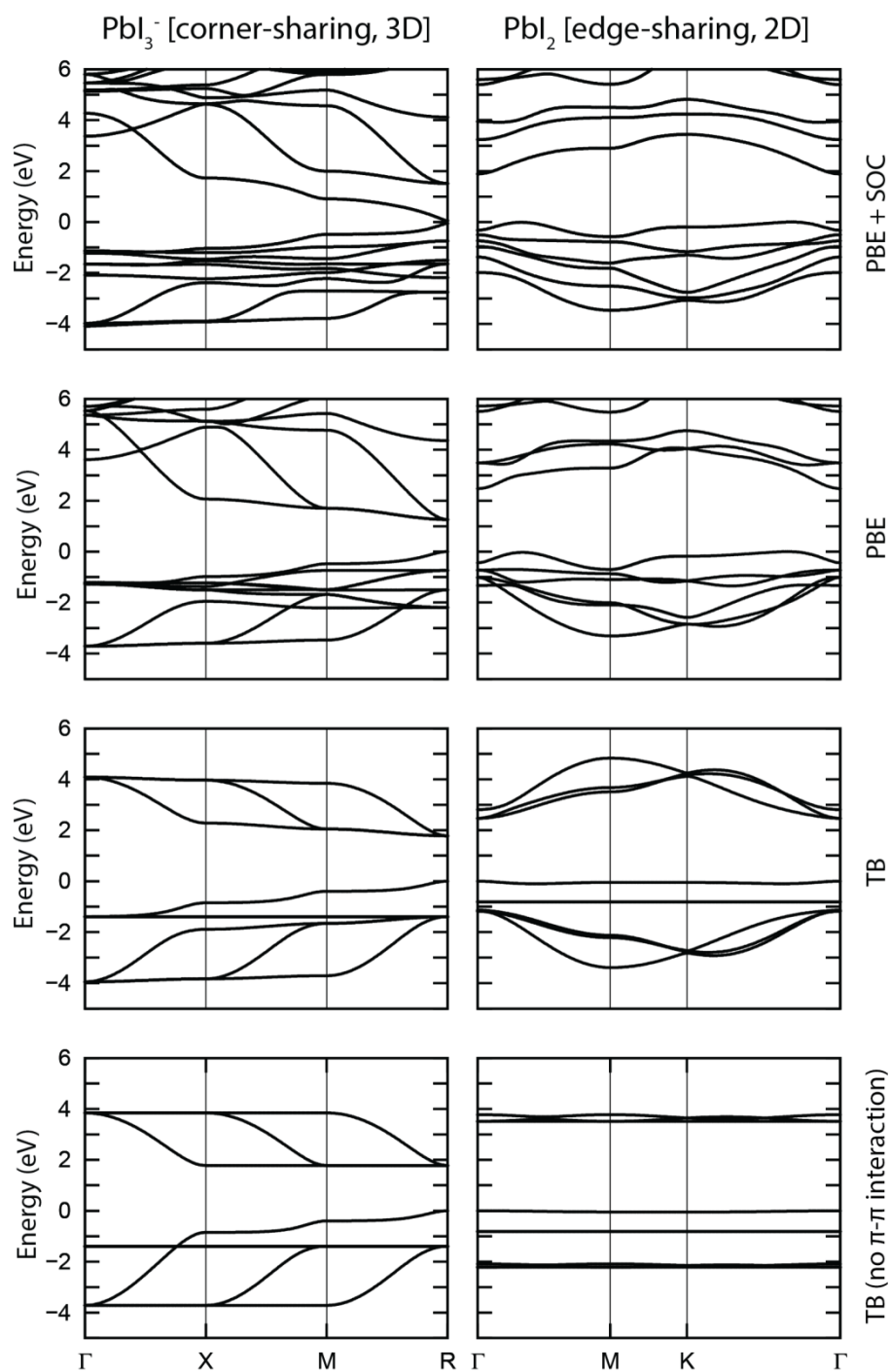
Figure S6. Comparison of the electronic band structures and tight-binding (TB) fits to the electronic band structures of theoretical models of 3D corner-sharing and 2D edge-sharing PbI_6 octahedra. From top to bottom: band structures using the PBE functional, with spin-orbit coupling (SOC), band structures without SOC, TB fit, and TB fit without including the π-π interaction.

In this TB approximation, only the nearest-neighbor interaction is considered. The TB fit includes *s-s* overlap, *s-p* interactions, *p-p* (σ-σ) interactions and *p-p* (π-π) interactions. The TB parameters (on-site energies, Slater-Koster parameters) were fitted for the 2D edge-sharing and 3D corner-sharing structures to approximate the DFT band structures as closely as possible. The final TB calculations were performed using the averaged parameters for both structures (see Table S1). For the TB calculations, the TBPW 1.1 program was used.[1] As can be seen in Figure S6, the TB fit describes the essence of the DFT band structures. Hopping of carriers from one Pb to another Pb is only possible via an intermediate I. In the case of the 3D corner-sharing structure, this means that all Pb-I-Pb angles equal 180°. In contrast, the 2D hexagonal edge-sharing structure contains no 180° paths, and all the Pb-I-Pb angles equal 90°. Surprisingly, our results show that to pass these 90° corners, the *s-p* interaction barely plays a role, while the combination of *p-p* (σ-σ) and *p-p* (π-π) is crucial. The bottom panel of Figure S6 shows that without *p-p* (π-π) interactions, the band structure of the edge-sharing structure becomes very flat, while the band-structure of the corner-sharing structure stays nearly the same. Therefore, we conclude that the π-π overlap plays a significant role in the band structure of edge-sharing PbI_6-octahedra. Furthermore, as the π-π interactions are generally much weaker than the σ-σ interactions, this means that the entire *p-p* interaction is crucial. Note that we used a certain level of approximation, which excludes several interactions and parameters, such as next-nearest neighbor interactions, differences in crystal field, spin-orbit coupling and octahedral tilting. However, we see that although switching on the π-π interaction leads to a significant band broadening, the gap for the hexagonal system remains larger than that of the cubic system. It is this, combined with the much stronger effect of SOC in the cubic system, that results in a significantly larger band gap in the hexagonal edge-sharing system.

Table S1. The average parameters (in eV) used in the TB calculations.

| Type	Value	Type	Value
Pb on-site *s*	-8.566875	*s-s*	-0.539441
Pb on-site *p*	0.3552425	*s-p*	0.926776
I on-site *s*	-12.7056765	*p-p* (σ-σ)	1.742416
I on-site *p*	-2.5597875	*p-p* (π-π)	-0.484158

Electronic band structure diagrams of all theoretical model structures.

Here, we present the electronic band structure diagrams of the 3D (corner-sharing), 2D (corner- and edge-sharing) and 1D (corner-, edge- and face-sharing) model structures, calculated within DFT, with and without spin-orbit coupling. We modeled the 2D slabs and 1D linear chains (see Figure S7) using a 3D periodically repeated super cell. We calculated the approximate band gaps by evaluating the band structures as a function of distance between the periodic image of the slabs or chains. When the distance is too small, undesired interactions between the slabs or chains occur. However, as most of the systems have a negative charge, electrons start to become unbound when the distance between the chains becomes too large, due to reduction of the positively charged background (negatively charged ions are often unstable in LDA and GGAs). As a result, vacuum levels can have a lower energy than the LUMO of the slabs or chains themselves. This can be accounted for when the band structures are calculated as a function of distance between the slabs or chains (Figures S9-S12). As an example, consider the case of Figure S10, top part. At small distance ($d = 10$ Å), the valence band top and conduction band minimum are not yet at the correct energies, as the influence from the periodic images is present. At larger distance, the occupied bands are practically independent of d and the valence band top is not affected by interactions with the periodic images anymore. For the empty states, the situation is a bit more complicated. The minimum at X moves down from $d = 10$ Å to $d = 11$ Å to $d = 12$ Å. From $d = 12$ Å, the position of this state hardly changes, i.e. the periodic images do not matter anymore. However, one can also see vacuum-like states. These are characterized by a strong dependence on d, see e.g. the empty states minimum at Γ moving down strongly. A complication arises at $d = 13$ Å, where at X, a "vacuum" band is very close to the valence band minimum at 2.21 eV and interacts with it. At $d = 14$ Å, the vacuum states are much deeper and the state at 2.21 eV is, again, almost a pure state of the chain.
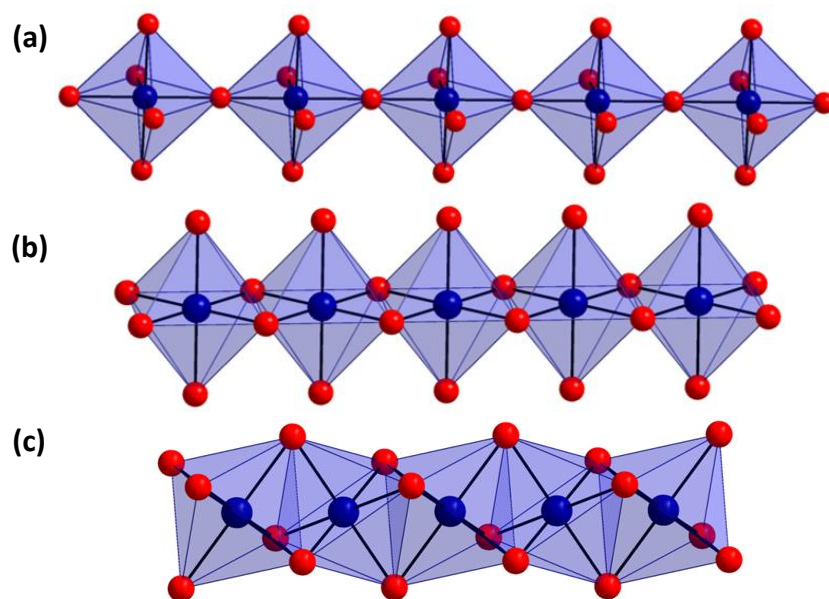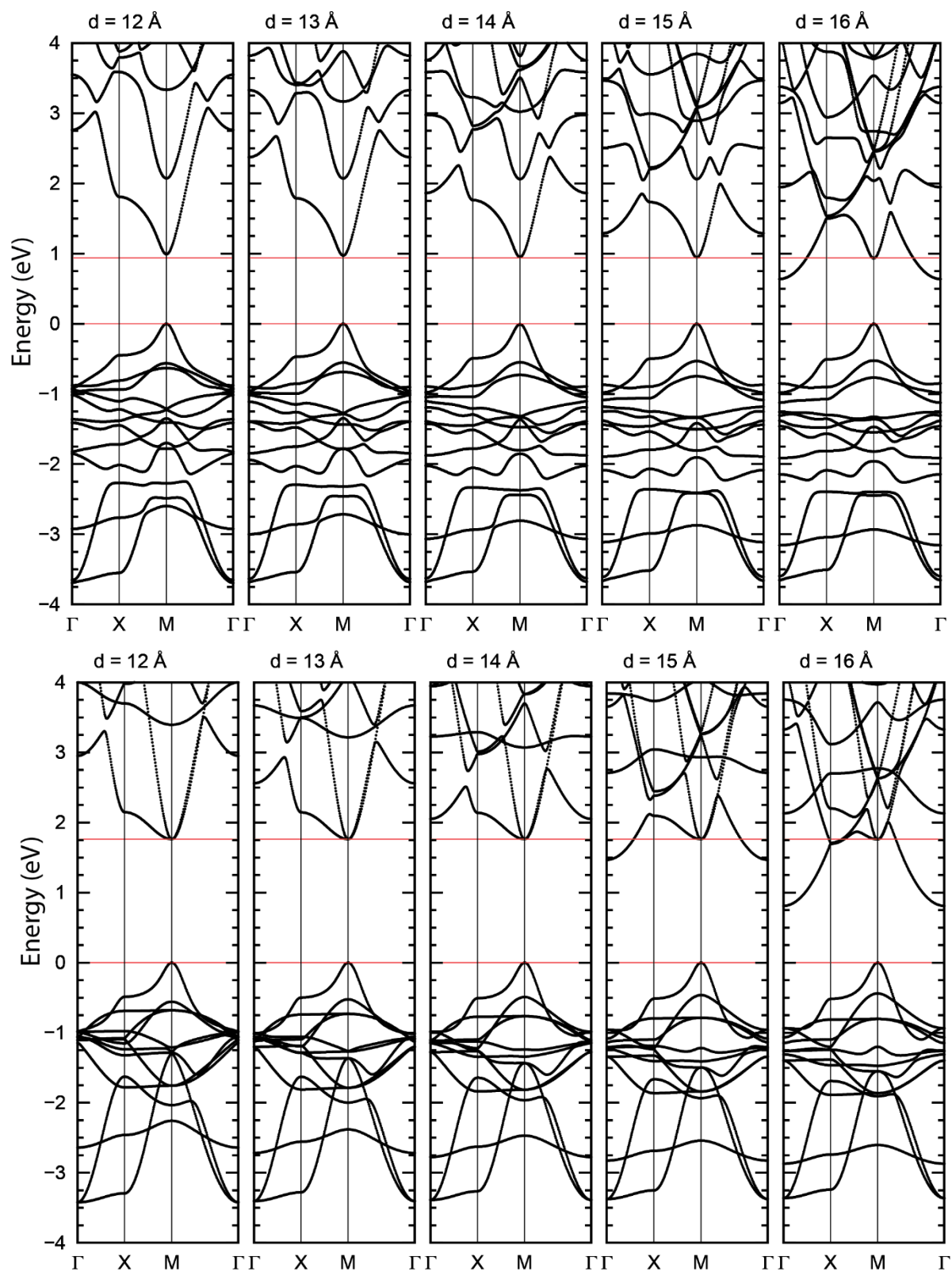
Figure S7. Polyhedral model of 1D linear chains of (a) corner-sharing, (b) edge-sharing and (c) face-sharing PbI_6 octahedra.
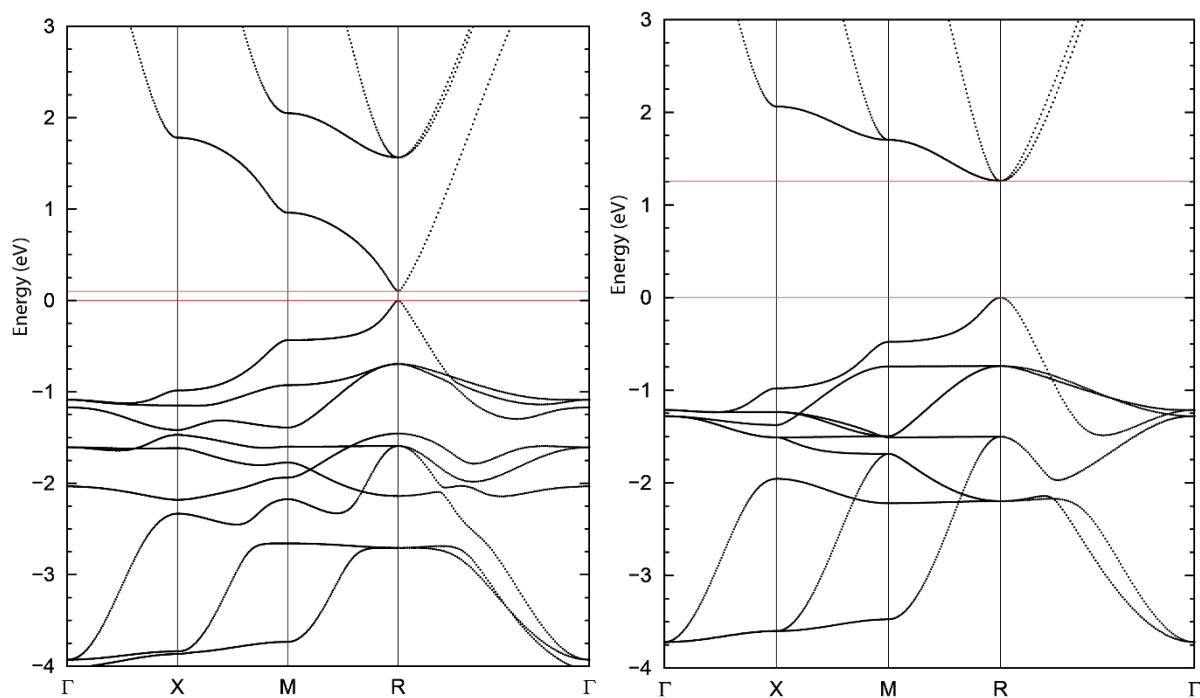
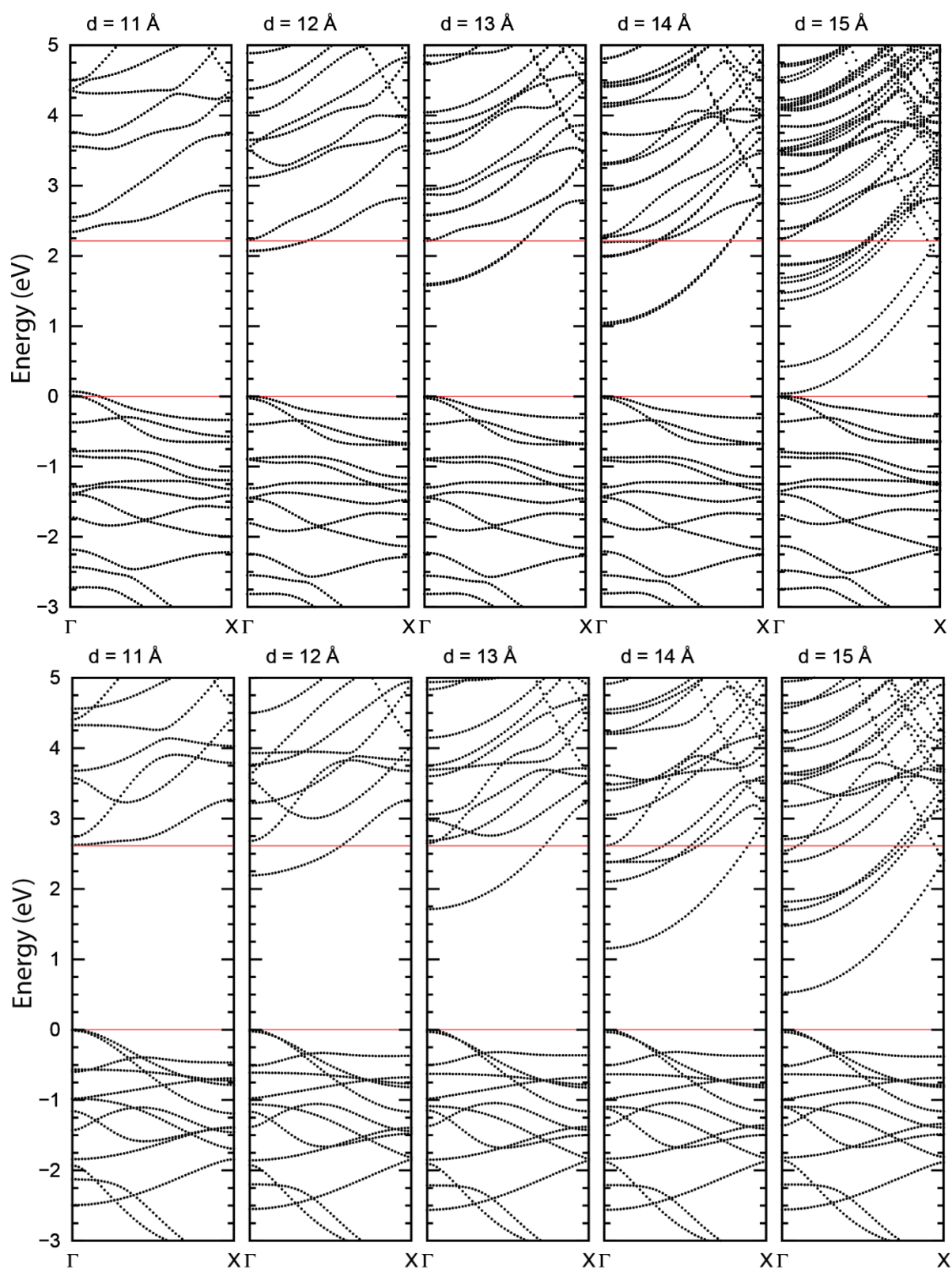**Figure S8.** Electronic band structure of 3D corner-sharing PbI_6 octahedra, composition $[PbI_3]^-$, calculated within PBE-DFT with SOC (left) and without SOC (right). Band gaps are 0.10 eV and 1.26 eV, respectively.

Figure S9. Electronic band structure of 2D corner-sharing PbI$_6$ octahedra, calculated within DFT with SOC (top) and without SOC (bottom), as a function of distance between the sheets. Approximate band gaps are 0.94 eV and 1.76 eV, respectively.
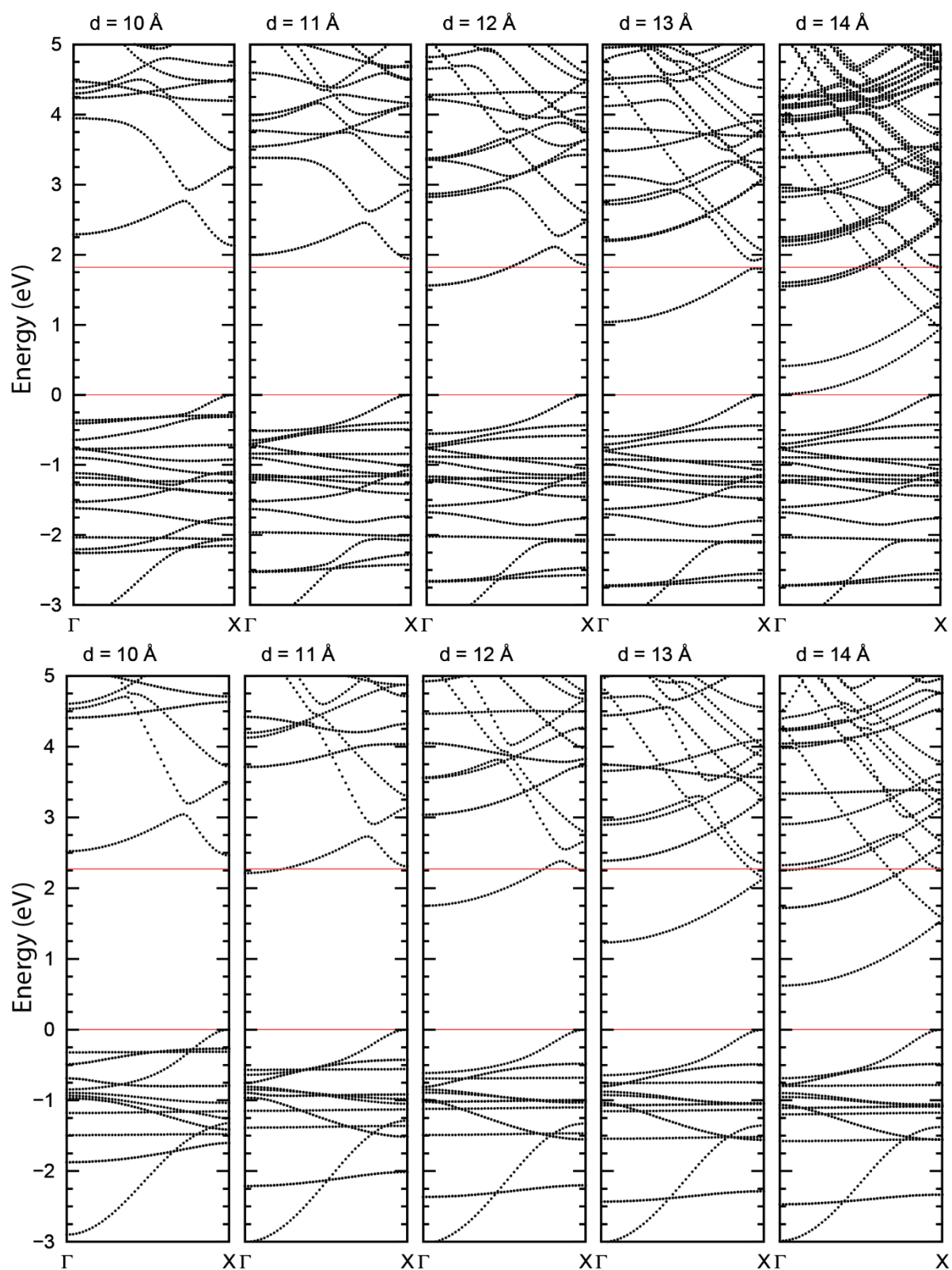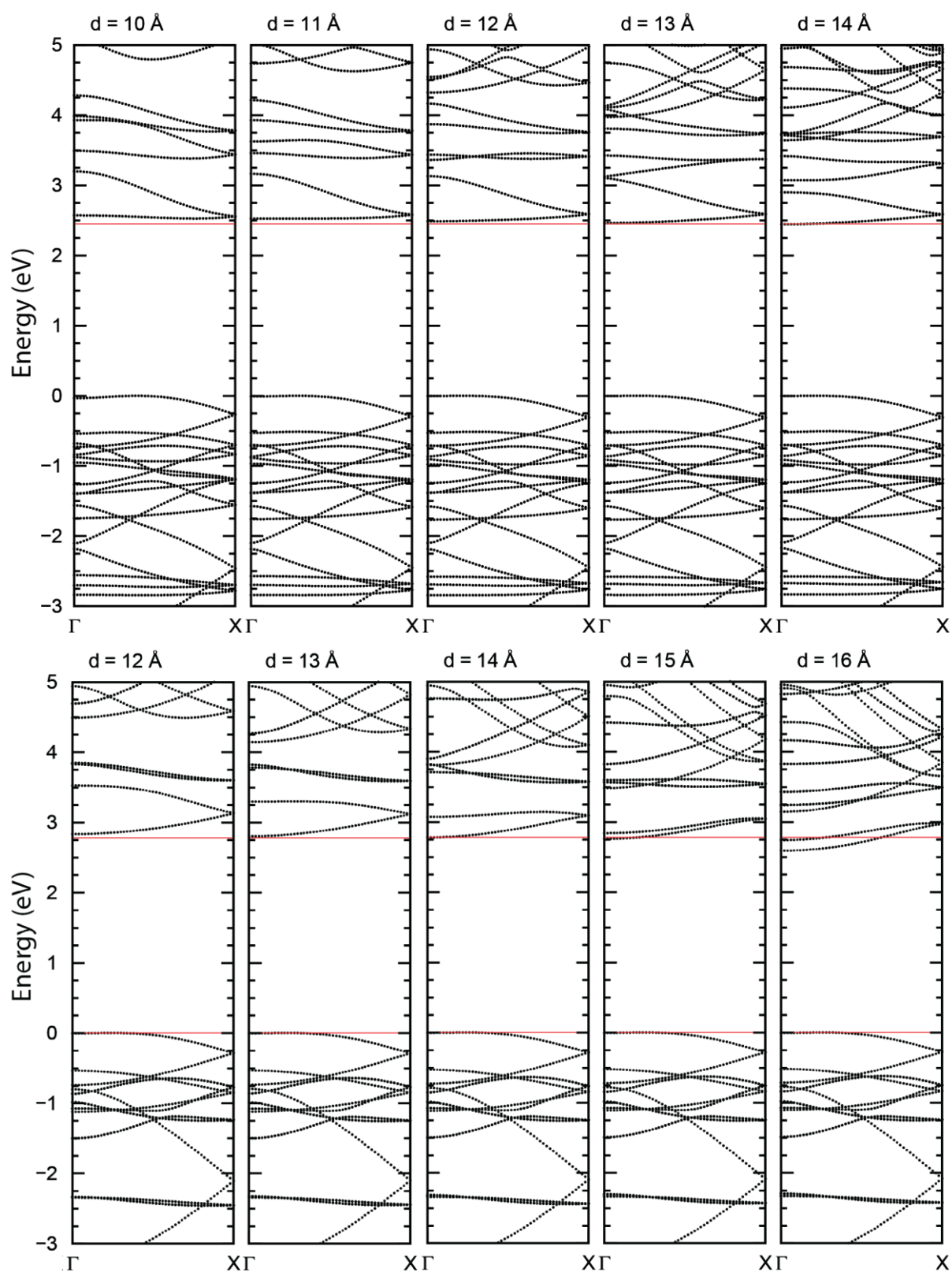
Figure S10. Electronic band structure of 1D corner-sharing PbI$_6$ octahedra, calculated within DFT with SOC (top) and without SOC (bottom), as a function of distance between the chains. Approximate band gaps are 1.82 eV and 2.27 eV, respectively.

Figure S11. Electronic band structure of 1D edge-sharing PbI_6 octahedra, calculated within DFT with SOC (top) and without SOC (bottom), as a function of distance between the chains. Approximate band gaps are 2.21 eV and 2.61 eV, respectively.

Figure S12. Electronic band structure of 1D face-sharing PbI$_6$ octahedra, calculated within DFT with SOC (top) and without SOC (bottom), as a function of distance between the chains. Approximate band gaps are 2.45 eV and 2.78 eV, respectively.

References

(1) Das, D.; Mattson, W.; Romero, N. A.; Martin, R. M. University of Illinois at Urbana-Champaign Materials Computation Center. **2004**.